

Novel physics opportunities at the HESR-Collider with PANDA at FAIR

Leonid Frankfurt¹, Mark Strikman², Alexei Larionov^{3,4,5},
Andreas Lehrach^{3,6}, Rudolf Maier^{3,6}, Hendrik van Hees⁷,
Christian Spieles⁷, Volodymyr Vovchenko^{5,7}, Horst Stoecker^{5,7,8}

¹*Sackler School of Exact Sciences, Tel Aviv University, Tel Aviv, Israel*

²*Pennsylvania State University, University Park, PA, USA*

³*Institut für Kernphysik, Forschungszentrum Jülich, D-52425 Jülich, Germany*

⁴*National Research Center “Kurchatov Institute”, 123182 Moscow, Russia*

⁵*Frankfurt Institute for Advanced Studies, Giersch Science Center,
D-60438 Frankfurt am Main, Germany*

⁶*JARA-FAME (Forces and Matter Experiments), Forschungszentrum Jülich
and RWTH Aachen University, Germany*

⁷*Institut für Theoretische Physik, Goethe Universität Frankfurt,
D-60438 Frankfurt am Main, Germany*

⁸*GSI Helmholtzzentrum für Schwerionenforschung GmbH,
D-64291 Darmstadt, Germany*

March 1, 2022

Abstract

Exciting new scientific opportunities are presented for the PANDA detector at the High Energy Storage Ring in the redefined $\bar{p}p(A)$ collider mode, HESR-C, at the Facility for Antiproton and Ion Research (FAIR) in Europe. The high luminosity, $L \sim 10^{31} \text{ cm}^{-2} \text{ s}^{-1}$, and a wide range of intermediate and high energies, $\sqrt{s_{NN}}$ up to 30 GeV for $\bar{p}p(A)$ collisions will allow to explore a wide range of exciting topics in QCD, including the study of the production of excited open charm and

bottom states, nuclear bound states containing heavy (anti)quarks, the interplay of hard and soft physics in the dilepton production, and the exploration of the regime where gluons – but not quarks – experience strong interaction.

1 Introduction

The experimental discovery of charmonium [1, 2] and bottomonium [3] in e^+e^- and pA collisions suggests that hadrons containing heavy quarks can be investigated in hadronic processes, where dense, strongly interacting medium could be formed. It can be particularly useful to study the annihilation of antiprotons on free protons and baryons bound in nuclei in $\bar{p}p(A)$ collisions, in both collider and fixed-target experiments at collision energies of $\sqrt{s} = 2\text{--}200$ GeV.

A unique opportunity to do this in the near future is provided by the Facility for Antiproton and Ion Research (FAIR), with the PANDA detector at the high-energy storage ring (HESR). This concerns both, the presently developed HESR fixed target mode at $\sqrt{s} < 6$ GeV, and a future collider mode at $\sqrt{s} < 32$ GeV, with PANDA as midrapidity detector. The collider mode would need just an injection-beam transfer line from the SIS 18 directly into HESR, as discussed in Ref. [4]. Additionally, asymmetric HESR collider schemes with somewhat lower center-of-mass energies have been discussed in detail [5, 6, 7]. It may also be feasible to study $\bar{p}A$ collisions for $\sqrt{s_{NN}}$ of up to 19 GeV with interesting physics opportunities [8, 9].

Luminosities of up to $5 \cdot 10^{31} \text{ cm}^{-2}\text{s}^{-1}$ can be reached at $\sqrt{s} \simeq 30$ GeV in the symmetric $\bar{p}p$ collider mode at the HESR [10, 11]. The collision scheme of twelve proton bunches colliding with the same amount of antiproton bunches has to be adapted to the HESR. This modification of the HESR requires a second proton injection, the Recuperated Experimental Storage Ring (RESR), the 8 GeV electron cooler and a modification of the PANDA interaction region.

Besides the deceleration of rare-isotope beams, the RESR storage ring also accumulates high-intensity antiprotons, via the longitudinal momentum stacking with a stochastic cooling system [12]. This is achieved by injecting and pre-cooling the produced antiprotons at 3 GeV in the Collector Ring (CR) storage ring.

The anticipated beam intensities in the HESR proton-antiproton collider

version require a full-energy electron cooler (8 MeV) to avoid beam emittance growth, which results in a decreased luminosity during the cycle. The Budker Institute of Nuclear Physics (BINP) presented a feasibility study for magnetized high-energy electron cooling. An electron beam up to 1 A, accelerated in dedicated accelerator columns to energies in the range of 4.5-8 MeV has been proposed. For the FAIR full version, it is planned to install the high-energy electron cooler in one of the HESR straight sections [13, 14, 15].

In the fixed-target mode, at $E_{\text{kin}} = 4\text{-}10$ GeV, it will be possible to perform complementary measurements of the cross section of charmonium interaction with nuclear matter with the PANDA detector.

A conservative estimate of the $p\bar{p}$ luminosities which can be reached at the startup phase without RESR is $4 \cdot 10^{30} \text{ cm}^{-2}\text{s}^{-1}$. We will use it below in our estimates assuming a one year run (10^7sec). Energies \sqrt{s} up to 30 GeV could be reached and it may also be feasible to study \bar{p} - heavy-nucleus collisions for $\sqrt{s_{NN}}$ of up to 19 GeV. In the present work we outline how the collider at the HESR machine will extend the scope of the PANDA project, with a focus on a few highlights. In Sections 2 and 3 we discuss the potential of the $\bar{p}p$ collider to provide new information in the field of heavy quark physics, with some attention devoted to the possible discovery of new states. Some other related opportunities are outlined in Sec. 4. Section 5 presents a number of additional physics topics that could be explored in both $\bar{p}p$ and $\bar{p}A$ modes. These include the production of nuclear fragments containing \bar{c} and/or c quarks, the $c\bar{c}$ pair production, color fluctuation effects, probing the pure glue matter, and the production of low-mass dileptons. Concluding remarks in Sec. 6 close the article.

2 Study of bound states containing heavy quarks

A number of new states containing heavy quarks have been discovered recently. These can be interpreted as pentaquark and tetraquark states containing $c\bar{c}$ pairs. Some of the states are observed in decays of mesons and baryons containing b-quarks, others in the final states of e^+e^- annihilation; for a review see [16].

It is widely expected that these discoveries represent just the start of the exploration of rich new families of states containing heavy quarks. Understanding the dynamics responsible for the existence of these states would help to clarify many unresolved issues in the spectroscopy of light hadrons.

A unique feature of an intermediate-energy $\bar{p}p$ collider is that it makes possible to study the production of $Q\bar{Q}$ ($Q = c, b$) pairs and the formation of various hadrons containing heavy quarks rather close to the threshold. The $b\bar{b}$ pairs are produced mostly in the process of annihilation of valence quarks and antiquarks, i.e. $q\bar{q} \rightarrow Q\bar{Q}$. The production of $c\bar{c}$ pairs in the antiproton fragmentation region also corresponds to this mechanism.

The invariant masses of the produced $Q\bar{Q}$ pairs are much closer to the threshold in the discussed energy range than at the LHC energies. It is natural to expect that the large probability to produce final states with small $Q\bar{Q}$ invariant masses should lead to a higher relative probability to produce pentaquark and tetraquark states compared to the one at the LHC energies. Additionally, the small transverse momenta of the $Q\bar{Q}$ pairs facilitate the pick up of light quarks as compared to Q or \bar{Q} fragmentation. In the antiproton-fragmentation region another $Q\bar{Q}$ production enhancement mechanism, specific for antiproton interactions, is possible: the production of $Q\bar{Q}$ pairs with large $x \sim 0.2-0.4$ in the annihilation of $q\bar{q}$, which could merge with a spectator antiquark of the antiproton carrying $x \sim 0.2$.

Another effect which can help to observe new states in medium-energy $\bar{p}p$ collisions is the relatively low spatial density of the system produced at moderate energies. This should suppress final-state interactions, which could possibly hinder the formation of weakly bound clusters of large size. An additional advantage is a relatively small bulk hadron production which reduces the combinatorial background significantly as compared to the LHC.

2.1 The heavy quark production rates

The need for $t\bar{t}$ -production cross sections has stimulated the development of new computational techniques for heavy-quark production in hadron-hadron collisions (see, e.g., Refs. [17, 18]), in particular those which include the effects of threshold resummation.

These calculations, which are currently being validated by comparison to data at high collision energies, predict the following cross section for the $b\bar{b}$ pair production in $\bar{p}p$ collisions [19]:

$$\sigma_{b\bar{b}}(\sqrt{s} = 30 \text{ GeV}) = 1.8 \cdot 10^{-2} \text{ } \mu\text{b.} \quad (1)$$

This calculation has a relative uncertainty of about 30%, and the predicted cross section value is about seven times higher than the corresponding cross

section for pp scattering because of the contribution of the valence-quark valence-antiquark annihilation present in $\bar{p}p$. The $b\bar{b}$ cross section per nucleon for the $15 \text{ GeV} \times 6 \text{ GeV}$ kinematics is a factor of 100 smaller. Charm production is dominated by gluon annihilation, $gg \rightarrow Q\bar{Q}$. This fact implies that the corresponding cross sections are close in pp and $\bar{p}p$ collisions, with the exception of the fragmentation regions. The experimental data in this case are rather consistent between pp and $\bar{p}p$ and correspond to

$$\sigma_{c\bar{c}} = 30 \mu\text{b}. \quad (2)$$

For the $15 \text{ GeV} \times 6 \text{ GeV}$ scenario the cross section per nucleon drops by a factor of 3.

2.2 Rate estimates

The cross sections in Eqs. (1) and (2) correspond to significant event rates for one year (10^7 s) of running at a luminosity of $4 \cdot 10^{30} \text{ cm}^{-2}\text{s}^{-1}$. We find

$$N_{b\bar{b}} = 10^6, \quad N_{c\bar{c}} = 10^9. \quad (3)$$

These numbers can be easily rescaled for a run at a different luminosity, if required.

At these energies a rearrangement of the light-quark fractions occurs in the final states without significant suppression since heavy quarks are dominantly produced at mid rapidity, and the interaction between a b quark and a light valence quarks produces slow light quarks. Thus the overlapping integral between such a $b\bar{q}$ pair and the corresponding hadron wave function should be large. Most likely mesons are produced in excited states. The probability for the formation of $b\bar{q}$ mesons with a given flavor is about 30% of the total cross section because of the competition between different flavors. In the discussed processes gluon radiation is a small correction because of the restricted phase space and the large b-quark mass.

At the collision energies considered here, the combinatorial background is significantly smaller compared to LHC energies, which makes the observation of the excited states containing heavy quarks easier. In particular, the spectator quarks and antiquarks will have quite small velocities relative to the b quark. Indeed, for $\sqrt{s} = 30 \text{ GeV}$ a typical x value for the b-quark is $m_b/\sqrt{s} \gtrsim 0.2$, which is close to the x values of the valence quarks. This fact suggests the possibility of formation of excited states in both the meson and

the baryon channels, as well as an enhanced probability of the production of the excited $b\bar{b}q\bar{q}$ tetraquark or $(b\bar{q}) - (\bar{b}q)$ mesonic molecular states.

2.3 Hidden beauty resonance production

In contrast to charm production, the cross section for hidden beauty resonance production $p\bar{p} \rightarrow \chi_b$ may be too low for the process to be observed at the HESR. Within the standard quarkonium models, where a $Q\bar{Q}$ pair annihilates into two gluons which subsequently fragment into light quarks, one can estimate that this cross section drops with M_Q as $R_{b/c} = \Gamma(\chi_b \rightarrow p\bar{p})/\Gamma_{\text{tot}}(\chi_b) \propto \alpha_s^8/M_Q^8$. This is because this cross section is proportional to the partial width of the decay $p\bar{p} \rightarrow \chi_b$, which drops with an increase of M_Q . The ratio of cross sections of beauty production through a χ_b intermediate state to that for charm is $\approx [\alpha_s(M_Q)/\alpha_s(M_c)]^8/[M_c/M_Q]^{10}$ with an additional factor of M_Q^{-2} stemming from the expression for the resonance cross section. The suppression is due to the necessity of a light-quark rearrangement in the wave function of the proton to obtain decent overlapping with χ_b states. In the non-relativistic approximation the wave functions of χ_b states vanish at zero inter-quark distance. Thus the overall suppression for the total cross section of χ_b production as compared to that of χ_c production is approximately 10^{-7} .

3 Potential for discovery of new states

Investigating $p\bar{p}$ collisions at moderate energies carries specific advantages for searches of new states as the $b\bar{b}$ -production rate is relatively high, while the overall multiplicity, which determines the background level, is rather modest. Also, an equal number of states containing quarks and antiquarks is produced enabling cross checks of observations using conjugated channels. In the following we will discuss resonances containing heavy quarks with the understanding that everything said equally applies to the resonances containing heavy antiquarks. Although the rates in many cases are rather modest, we nevertheless include the discussion of these channels in view of the possibility to have a higher energy collider, as discussed in the final remarks (Sec. 6).

3.1 bqq -baryons and $b\bar{q}$ mesons

The current knowledge of the spectrum of the excited states containing b - or \bar{b} -quarks is very limited. According to PDG [20], in the $q\bar{b}$ sector there are two states $B_J(5970)^+$ and $B_J(5970)^0$ with unknown quantum numbers which could be excited states of the B^+ and B^0 , respectively. In the bqq -sector there are two baryons $\Lambda_b(5912)^0$ and $\Lambda_b(5920)^0$ which can be regarded as orbitally excited states of Λ_b^0 and one excited Σ_b^* state. This is much less in comparison with the cqq sector where five excited Λ_c^+ states and two excited Σ_c states (all rated with ***) are observed.

So there are plenty of opportunities here. One noteworthy issue is the comparison of the accuracy with which the heavy-quark limit works for hadrons containing b quarks vs. those containing c quarks.

3.2 Excited states containing $b\bar{b}$

As argued above it is very difficult to produce bound states containing $b\bar{b}$ in the resonance process of $p\bar{p}$ annihilation. Nevertheless, many of these states, as well as other states like analogs of X, Y, Z charmonium states, could be produced in inelastic $p\bar{p}$ interactions. This is because the invariant mass of the produced $b\bar{b}$ system is rather close to the threshold, and because the $b\bar{b}$ pair is produced in association with several valence quarks and valence antiquarks which have rather low momenta relative to the $b\bar{b}$ pair.

3.3 Baryons and mesons containing two heavy quarks

Since there are three valence antiquarks colliding with three valence quarks in $p\bar{p}$, one can produce two pairs of heavy quarks in a double quark-antiquark collision. This entails a possibility for producing the following baryons and mesons containing two heavy quarks:

(i) *ccq baryons.*

At the collision energies discussed, the contribution of the leading-twist mechanism of $2g \rightarrow Q\bar{Q}Q\bar{Q}$ for the double heavy-quark production should be quite small as it requires very large x of the colliding partons (the situation might be less pronounced for the case of the double $c\bar{c}$ production than for $b\bar{b}$). Therefore, the only effective mechanism left is the production of two pairs of heavy quarks in two hard parton-parton collisions (see Fig. 1).

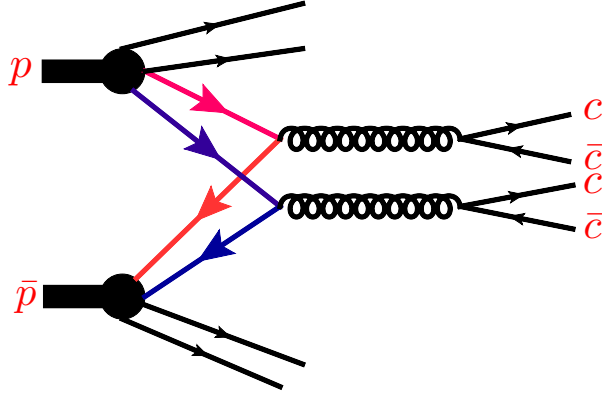


Figure 1: Double parton interaction mechanism for the production of two pairs of heavy quarks.

For the case of double $c\bar{c}$ pair production, one can make estimates by considering the suppression factor for the production of the second $c\bar{c}$ pair relative to a single $c\bar{c}$ pair. This factor can be roughly estimated using the high-energy experimental studies of double-parton collisions at the Tevatron collider. One finds a probability of about 10^{-3} for the ratio of the cross section for producing two $c\bar{c}$ pairs relative to a single pair. (To be conservative we took a factor of two smaller value of the parameter which determines the probability of double collisions ($1/\sigma_{\text{eff}}$) than the one measured at Tevatron as in the Tevatron kinematics special small- x effects may enhance this factor.) These considerations result in

$$N_{c\bar{c},c\bar{c}} = 10^6 \quad (4)$$

as an estimate for the yearly number of events with two pairs of $c\bar{c}$. Since the available phase space is rather modest, there is a significant probability that the relative velocity of two c - quarks would be small, and therefore a ccq state would be formed.

Other interesting channels are production of an open charm-anticharm pair plus charmonium, and double charmonium.

(ii) bcq baryons and $b\bar{c}$ mesons.

The $b\bar{b}c\bar{c}$ pairs are produced pretty close to threshold and have small relative velocities. Hence there is a good chance that they would form a bcq baryon. About 10^3 events per year of running with $b\bar{b}c\bar{c}$ could be expected based on the double parton interaction mechanism.

(iii) *bbq baryons.*

To observe the production of $\sim 10^2$ $b\bar{b}b\bar{b}$ pairs one would need a one-year run at a much higher luminosity of 10^{33} $\text{cm}^{-2}\text{s}^{-1}$. The velocities of two b quarks are expected to be close in about 1/2 of the events. So there should be a significant chance for them to form bbq baryons.

(iv) *bcc baryons.*

Whether it is feasible to observe bcc states requires more detailed estimates and may depend on the structure of the three-quark configurations in the nucleon. A naive estimate is that 10^2 events with $bcc\bar{b}\bar{c}\bar{c}$ would be produced in a one-year run at a higher luminosity of 10^{33} $\text{cm}^{-2}\text{s}^{-1}$.

Note also that even though a $b\bar{c}$ meson has been observed (although its quantum numbers are not known), there are potentially many other states built of these quarks suggesting a rich spectroscopy (mirroring the spectra of $c\bar{c}$ - and $b\bar{b}$ -onium states).

3.4 Summary

To summarize, it would be possible with PANDA at the HESR-C $\bar{p}p$ collider to discover and to study properties of meson and baryon states containing one b quark and light (anti) quarks, complementing the charmonium states which are planned to be explored in the PANDA fixed target experiment. There are also good chances to discover the double-heavy-quark baryonic and mesonic states. These new potential observations will allow to achieve a much deeper understanding of the bound-state dynamics in QCD.

4 Other opportunities

In the last decades much effort has been devoted to studying high-energy properties of QCD in the vacuum channel - the so called perturbative Pomeron. Interactions in non-vacuum channels, on the other hand, have practically not been studied. The PANDA experiment at a collider has a perfect kinematic coverage to study the behavior of Regge trajectories in both the non-perturbative regime (small Mandelstam t) as well as the possible onset of the perturbative regime. One advantage of the antiproton beam is the possibility to study a wide range of baryon and meson Regge trajectories, possibly including Regge trajectories with charmed quarks. The latter will allow to

check the non-universality of the slopes of the Regge trajectories which were observed already at positive t values.

Other possibilities include Drell-Yan-pair measurements, which at the lower end of the discussed energy range, may be extended to the limit of exclusive processes like $\bar{p}p \rightarrow \mu^+\mu^- + \text{meson}$ which are sensitive to generalized parton-distribution functions, etc.

Another direction of studies is the investigation of correlations between valence (anti)quarks in (anti)nucleons using multi-parton interactions (MPI) analogous to those shown in Fig. 1. In the discussed energy range MPI get a significant contribution from collisions of large- x partons (double Drell-Yan, Drell-Yan + charm production, etc.), and the rate of the MPI is inversely proportional to the square of the average distance between the valence quarks. In particular the rates would be strongly enhanced in the case of a large probability of (anti)quark-(anti)diquark configurations in the (anti)nucleon.

The analysis of the production of heavy-quark pairs discussed above would also be of great interest for the study of the multiparton structure of nucleons.

4.1 $\bar{p}A$ elastic scattering and absorption

So far measurements of the antiproton-nucleus elastic scattering were done only at LEAR for $p_{\text{lab}} < 1 \text{ GeV}/c$. It turned out that owing to the forward-peaked $\bar{p}p$ elastic scattering amplitude the Glauber model describes LEAR data on the angular differential cross sections of $\bar{p}A$ elastic scattering surprisingly well. This is in contrast to the pA elastic scattering where the Glauber model description starts to work only above $p_{\text{lab}} \sim 1.5 \text{ GeV}/c$ [21].

Glauber theory analysis [22] has shown that the $\bar{p}A$ and pA angular differential elastic scattering cross sections at $p_{\text{lab}} = 10 \text{ GeV}/c$ (fixed target PANDA) strongly differ in the diffraction minima due to the different ratios of the real-to-imaginary parts of $\bar{p}N$ and pN elastic scattering amplitudes. Experimental confirmation of such a behavior would be a good validity test of the Glauber theory, important in view of its broad applications for other reaction channels, and of the input elementary amplitudes which are typically given by Regge-type parameterizations. In particular, the $\bar{p}n$ elastic amplitude is accessible only by scattering on complex nuclei. The determination of diffractive structures at $\bar{p}A$ -collider energies would require good transverse momentum transfer resolution $\sim 10 \text{ MeV}/c$ and the capability to trigger on the events where nucleus remains intact (see the discussion in Sec. 5.2). Light

nuclear targets are preferred as their diffractive structures are broader in p_t , and there is a smaller number of possible excited states. Spin 0 targets like ${}^4\text{He}$ are especially good for these purposes.

A related problem is the determination of the antiproton absorption cross on nuclei (defined as the difference between total and elastic cross sections). Experimental data on the antiproton absorption cross section above LEAR energies are quite scarce, although such data are needed for cosmic ray antiproton flux calculations [23].

4.2 Coherent hypernuclei production

While ordinary Λ -hypernuclei were discovered long ago, the Λ_c^+ - and Λ_b^0 -hypernuclei were predicted in mid-70s [24, 25] but have not been observed so far. However, their existence is expected based on a number of models, e.g the quark-meson coupling model [26].

The processes $\bar{p}p \rightarrow \bar{Y}Y$, where $Y = \Lambda, \Lambda_c^+$ or Λ_b^0 , have the lowest thresholds among all possible other channels of the respective $\bar{s}s$, $\bar{c}c$ or $\bar{b}b$ production channels in $\bar{p}p$ collisions. Thus, they are preferred for Y -hypernuclei production as the momentum transfer to the hyperon is relatively small.

The coherent reactions ${}^AZ(\bar{p}, \bar{\Lambda})_{\Lambda}^A(Z-1)$ for the different states of the hypernucleus have never being studied experimentally. It is expected that these reactions have cross sections of the order of a few 10nb at $p_{\text{lab}} \sim 20 \text{ GeV}/c$ [27]. Thus, they can serve as a powerful source of Λ -hypernuclei production at the lower end of the $\bar{p}A$ -collider energies. Here, the amplitude $\bar{p}p \rightarrow \bar{\Lambda}\Lambda$ should be dominated by the K^* (or K^* Regge trajectory) exchange.

More challenging is the coherent process ${}^AZ(\bar{p}, \bar{\Lambda}_c^-)_{\Lambda_c^+}^AZ$ [28] where the underlying $\bar{p}p \rightarrow \bar{\Lambda}_c^- \Lambda_c^+$ amplitude is due to D^0 and D^{*0} exchanges. One can also think of the ${}^AZ(\bar{p}, \bar{\Lambda}_b^0)_{\Lambda_b^0}^A(Z-1)$ coherent reaction.

5 Unique opportunities for probing QCD properties at the $\bar{p}A$ collider

5.1 Space-time picture of the formation of hadrons containing heavy quarks

The kinematics of heavy-quark-state production in collisions of $p(\bar{p})$ with proton or nuclei (neglecting Fermi motion effects) dictates that heavy states can only be produced with momenta

$$p_Q > M_Q^2/2m_Nx_q - m_Nx_q/2 \quad (5)$$

in the rest frame of the nucleus. Here x_q is the x of the quark of the nucleus involved in the production of the $Q\bar{Q}$ pair. For $x_q \leq 0.5$ this corresponds to a charm momentum above $4 \text{ GeV}/c$ which is much larger than typical momenta of the heavy system embedded in the nucleus.

However, there is a significant probability that D, Λ_c, \dots hadrons slow down due to final-state interactions. Indeed, it is expected in QCD that the interaction strength of a fast hadron with nucleons is determined by the area in which the color is localized. For example, $\psi'-N$ interactions should be comparable to the kaon-nucleon cross section and be much larger than the $J/\psi-N$ cross section, see for example [29]. Also the cross sections of open charm (bottom) interactions should be on the scale $\gtrsim 10 \text{ mb}$.

The formation distance (coherence length) can be estimated as

$$l_{\text{coh}} \simeq \gamma l_0, \quad (6)$$

where $l_0 \simeq 0.5\text{-}1.0 \text{ fm}$. For the discussed energies and the case of scattering off heavy nuclei the condition

$$l_{\text{coh}} \leq R_A, \quad (7)$$

is satisfied for hadrons produced in a broad range of momenta including the central and nucleus fragmentation region. So it would be possible to explore the dependence of the formation time and interaction strength on, for example, the orbital angular momentum of D^* .

Observing these phenomena and hence exploring QCD dynamics in a new domain could be achieved by studying the A -dependence of charm production at momenta $\lesssim 10 \text{ GeV}/c$ (in the rest frame of the nucleus).

5.2 New heavy-quark states

The formation of heavy mesons or baryons, H , inside nuclei implies final-state interactions which slow down these heavy hadrons, leading to the production of hadrons at low momenta forbidden for scattering off a free proton:

$$p_H \leq (m_H^2 - m_N^2)/2m_N. \quad (8)$$

In this kinematics the slow-down may be sufficient to allow for the production of (anti-)charm quarks embedded in nuclear fragments. The collider kinematics would make it easier to detect decays of such nuclei than in fixed-target set ups as these nuclei would be produced with high momenta (velocities comparable to those of ordinary nuclear fragments). Thus the discussed HESR-C collider in the $\bar{p}A$ mode would have a high discovery potential for observing various nuclear states containing c and/or \bar{c} .

Higher luminosities and higher collider energies will allow search for analogous b and/or \bar{b} states.

5.3 Color fluctuations in nucleons

At high energies hadrons are thought to be interacting with each other in frozen configurations which have different interaction strengths – so-called color fluctuations. One can explore these phenomena in proton-nucleus collisions in a number of ways. Here we give as one example the study of the interaction strength of a hadron in the case of a configuration that contains a large- x ($x \geq 0.4$) parton. One expects that in such configurations the average interaction strength is significantly smaller than on average: in these configurations color screening leads to a suppression of the gluon fields and of the quark-antiquark sea [30]. This picture has allowed to explain [31, 32] strong deviations of the centrality dependence of the leading-jet production from the geometrical picture (Glauber model of inelastic collisions) observed at the LHC in p-Pb collisions and at RHIC in d-Au collisions.

Due to a fast increase of the interaction strength for small-size configurations with increasing energy, the strength of color fluctuations drops at higher energies. Correspondingly color-fluctuation effects are expected to be much enhanced at the HESR-C $\bar{p}A$ -collider energies. For example, for $x \simeq 0.6$, the cross-section ratio, $\sigma_{\text{eff}}(x)/\sigma_{\text{tot}}(NN)$, is expected to be ~ 0.25 , while at the LHC it is ~ 0.6 .

To observe this effect one would need to study Drell-Yan production at large x . A strong drop of hadron production in the nucleus fragmentation region would be a strong signal for the discussed effect. For its detailed study measurements with different nuclei would be desirable.

5.4 Probing pure glue matter

One of the central questions in high-energy hadronic and nuclear collisions is how the initially non-equilibrium system evolves towards a state of apparent (partial) thermodynamic equilibrium at later stages of nuclear collisions. Presently, the community favors a paradigm of an extremely rapid (t_{eq} less than $0.3 \text{ fm}/c$) thermalization and chemical saturation of soft gluons and light quarks.

The large gluon-gluon cross sections lead to the idea [33] that the gluonic components of colliding nucleons interact more strongly than the quark-antiquark ones. The two-step equilibration scenario of the quark-gluon plasma (QGP) was proposed in [34, 35, 36]. It was assumed that the gluon thermalization takes place at the proper time $\tau_{\text{g}} < 1 \text{ fm}/c$ and the (anti)quarks equilibration occurs at $\tau_{\text{th}} > \tau_{\text{g}}$. The estimates of Refs. [37, 38, 39] show that τ_{th} can be of the order of $5 \text{ fm}/c$.

Recently the *pure glue* scenario was proposed for the initial state at midrapidity in Pb+Pb collisions at Relativistic Heavy Ion Collider (RHIC) and Large Hadron Collider (LHC) energies [40, 41]. According to lattice-QCD calculations [42], quarkless purely gluonic matter should undergo a first-order phase transition at a critical temperature $T_c = 270 \text{ MeV}$. At this temperature the deconfined pure glue matter transforms into the confined state of pure Yang-Mills theory, namely into a glueball fluid. This is in stark contrast to full QCD equilibrium with (2+1) flavors, where a smooth crossover transition takes place (see Fig. 2 for a comparison of the corresponding equations of state).

At $\sqrt{s_{NN}} \simeq 30 \text{ GeV}$ $\bar{p}p(A)$ collisions can create only small systems. Baryon free matter can be expected if the $\bar{p}p$ annihilation occurs briefly in the initial stage of the collision. An enhanced annihilation probability can be expected in $\bar{p}A$ collisions over the $\bar{p}p$ collisions. Therefore, the properties of this baryon-free matter can potentially be studied by looking into the difference in observables between $\bar{p}p(A)$ and $pp(A)$ at the same energy.

If indeed a hot thermalized gluon fluid, initially containing no (anti)quarks, is created in the early stage of a $\bar{p}p$ or $\bar{p}A$ collision at mid rapidity, it will

quickly cool and expand until it reaches a mixed-phase region at $T = T_c^{\text{YM}}$. After the initial pure gluon plasma has completely transformed into the glueball fluid, the system will cool down further. These heavy glueballs produced during the Yang-Mills hadronization process where the pure glue plasma forms a glueball fluid. The heavy glueballs will later evolve into lighter states, possibly via a chain of two-body decays [43], and finally decay into hadronic resonances and light hadrons, which may or may not show features of chemical equilibration.

Of course, a more realistic scenario must take into account that some quarks will be produced already before and during the Yang-Mills driven first-order phase transition. This scenario can be modeled by introducing the time-dependent effective number of (anti)quark degrees of freedom, given by the time-dependent absolute quark fugacity λ_q [44]:

$$\lambda_q(\tau) = 1 - \exp\left(-\frac{\tau_0 - \tau}{\tau_*}\right). \quad (9)$$

Here τ_* characterizes the quark chemical equilibration time.

To illustrate the above considerations, we apply the (2+1)-dimensional relativistic hydrodynamics framework with a time-dependent equation of state, developed in Refs. [45, 46] and implemented in the vHLLE package [47], to $p\bar{p}$ collisions at HESR. The equation of state interpolates linearly between the lattice equations of state for the purely gluonic Yang-Mills (YM) theory [42] $P_{\text{YM}}(T)$ at $\lambda_q = 0$ and the full QCD with (2+1) quark flavors [48] $P_{\text{QCD}}(T)$ at $\lambda_q = 1$:

$$\begin{aligned} P(T, \lambda_q) &= \lambda_q P_{\text{QCD}}(T) + (1 - \lambda_q) P_{\text{YM}}(T) \\ &= P_{\text{YM}}(T) + \lambda_q [P_{\text{QCD}}(T) - P_{\text{YM}}(T)]. \end{aligned} \quad (10)$$

$P_{\text{YM}}(T)$ and $P_{\text{QCD}}(T)$ are shown in Fig. 2.

The hydrodynamic simulations of $p\bar{p}$ collisions at $\sqrt{s} = 32$ GeV discussed below assume a hard-sphere initial energy density profile with radius $R = 0.6$ fm. The normalization of the energy is fixed in order to yield an initial temperature of 273 MeV in the central cell, which is slightly above the critical temperature of 270 MeV. This choice is motivated by Bjorken model based estimates at $\sqrt{s} = 30$ GeV for small systems [49].

Figure 3 (a) shows the τ -dependence of the temperature in the central cell for different quark equilibration times: $\tau_* = 0$ (instant equilibration), 1 fm/c

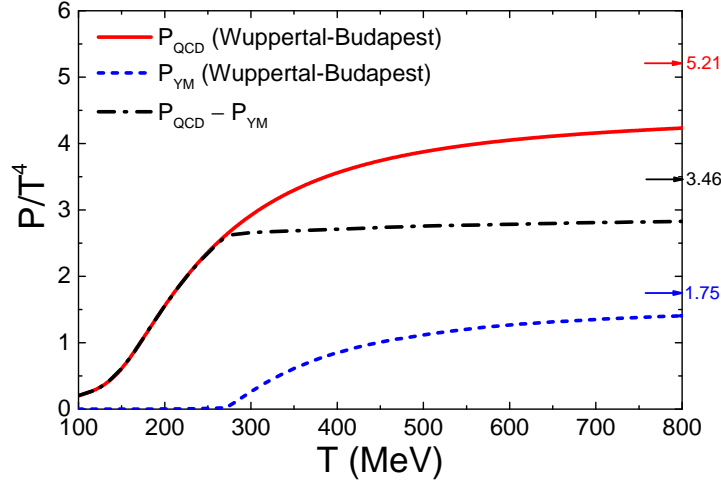


Figure 2: Temperature dependence of the scaled pressure p/T^4 obtained in lattice QCD calculations of the Wuppertal-Budapest collaboration for (2+1)-flavor QCD [48] (red line) and for Yang-Mills matter [42] (blue line). The black dash-dotted line depicts the difference between the pressure in full QCD and in Yang-Mills theory.

(fast equilibration), 5 fm/ c (moderate equilibration), 10 fm/ c (slow equilibration), and $\tau_* \rightarrow \infty$ (pure gluodynamic evolution). In the pure gluodynamic scenario, $\tau_* \rightarrow \infty$, the system spends a very long time in the mixed-phase region. A fast quark equilibration shortens the time period spent in the mixed phase significantly. Nevertheless, a significant fraction of the system evolution takes place in the mixed phase of the gluon-gluon deconfinement phase transition even at presence of a moderately fast quark equilibration ($\tau_* = 5$ fm/ c), as illustrated by Fig. 3b. Thus, significant effects of the initial pure glue state on electromagnetic and hadronic observables are expected for this collision setup.

These results illuminate the future HESR-collider option with the central PANDA experiment detector as an exciting upgrade for FAIR, a promising option to search for even heavier glueballs and hadrons than envisioned for the fixed target mode, and for other new exotic states of matter.

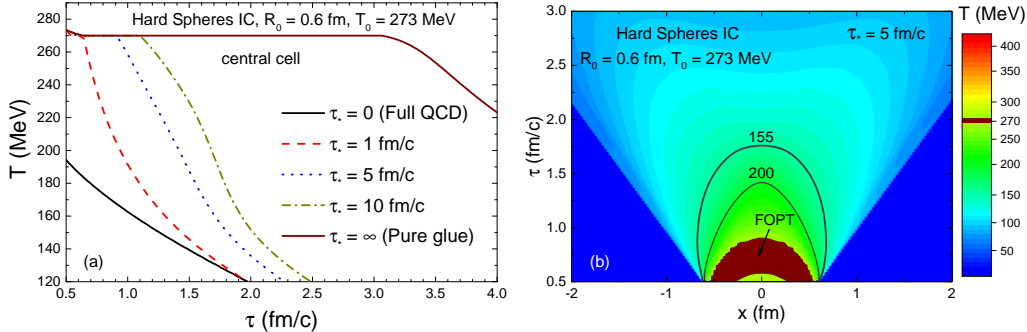


Figure 3: The temperature profile of the central cell in the longitudinally boost invariant (2+1)-dimensional hydro evolution for $p\bar{p}$ collisions in the pure glue initial state, the Yang-Mills scenario. A hard spheres overlap, transverse density profile with radius $R = 0.6$ fm is used as the initial condition. The normalization is fixed in order to yield the initial temperature of 273 MeV in the central cell. (a) The τ -dependence of the temperature is given for the central cell for different quark equilibration times: $\tau_* = 0$ (instant equilibration), 1 fm/c (fast equilibration), 5 fm/c (moderate equilibration), 10 fm/c (slow equilibration), and for $\tau_* \rightarrow \infty$ (pure gluodynamic evolution). (b) The temperature profile in the $x - \tau$ plane for $\tau_* = 5$ fm/c.

5.5 Low- and large mass dilepton production

Low-mass lepton pair production has raised the interest in the field for decades. A quite robust theoretical understanding [50, 51, 52, 53, 54, 55] of dilepton production in heavy-ion collisions at various energies has been gained. There dileptons play a special role as messengers from the early stages, as penetrating probes.

At large invariant dilepton masses the perturbative Drell-Yan (DY) mechanism of QCD sets in. The minimal M_{DY}^2 value, where the DY mechanism dominates, is not well known as it is difficult to separate it experimentally from the contribution of charm and J/ψ production. It seems that the DY pair production mechanism dominates at $M_{\text{DY}} \geq 2$ GeV. For $p\bar{p}(A)$ at intermediate energies, M_{DY} should be lower than for proton projectiles due to presence of abundant valence antiquarks.

Higher twist mechanisms may delay the inset of the leading-twist contribution in the case of interactions with nuclei. Drell-Yan production of dileptons at intermediate invariant masses by reactions with secondary mesons

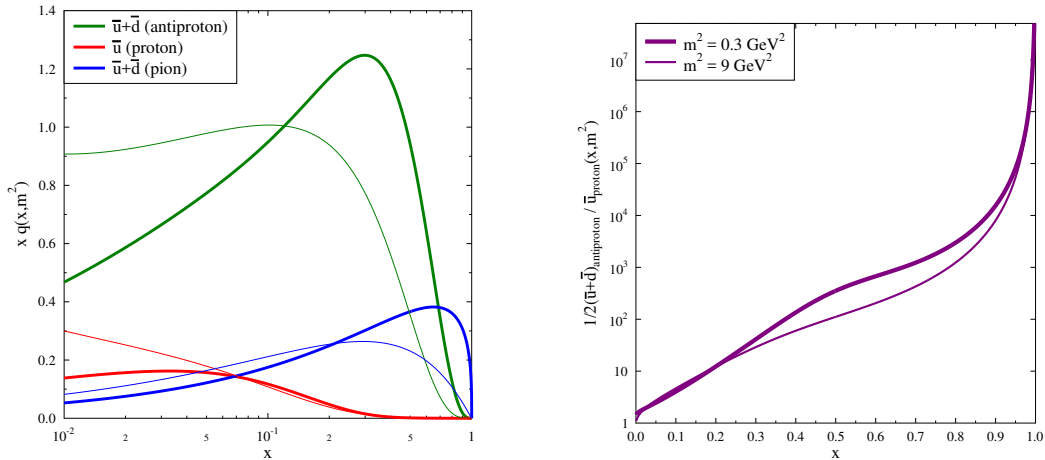


Figure 4: Left: The light-anti-quark parton-distribution functions (PDFs) at $m^2 = 0.3 \text{ GeV}^2$ (thin lines) and $m^2 = 9 \text{ GeV}^2$ (bold lines) for anti-protons, protons [56], and pions [57]. Right: The ratio of the PDFs for light anti-quarks in anti-protons and in protons.

and (anti-)baryons in pA and AA collisions has been investigated in [58, 59]. At the lower beam energies of the beam-energy scan at RHIC, at FAIR, and at NICA, strong contributions from secondary DY processes are predicted for low- and intermediate-mass dilepton pairs due to the formation of mesons at time scales $\lesssim 1 \text{ fm}/c$, i.e. during the interpenetration stage of projectile and target. This implies that inflying primordial projectile and target nucleons from the interpenetrating nuclei collide with just newly formed mesons (e.g., ρ and ω with constituent-quark and constituent-antiquark masses of $\sim 300 \text{ MeV}$ each).

For $\bar{p}p$ and $\bar{p}A$ reactions, the Drell-Yan production is enhanced already for the primordial collisions due to the presence of *valence* antiquarks of the antiproton, as displayed in Fig. 4 which shows the ratio of light-antiquark PDFs in antiprotons and protons. With the HESR-C $\bar{p}p$ and $\bar{p}A$ collider discussed here a direct assessment of the valence-quark valence-antiquark parton distributions in $\bar{p}p$ and $\bar{p}A$ collisions is accessible. The comparison of dilepton production by proton and antiproton induced reactions provides unique information on the relative role of initial- and final-state mechanisms. In particular, by comparing dilepton production in proton and antiproton fragmentation regions one may expect the maximal difference between the two cases.

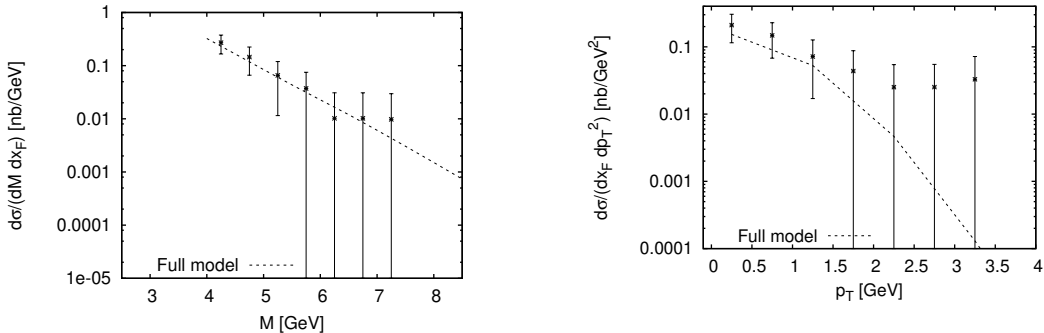


Figure 5: Invariant-mass (left) and transverse-momentum spectra (right) of DY dimuon pairs in $\bar{p}W$ at $\sqrt{s} = 15\text{GeV}^2$ collisions. Data are from the E537 collaboration [61]. The used integrated PDF's are the MSTW2008LO68cl set [63].

Calculations of the inclusive (integrated over transverse momenta) DY production can be performed now in the NNLO DGLAP approximation. The techniques were developed for calculations of transverse momentum distributions which include effects of multiple gluon emissions (the Sudakov form factor effects) and nonperturbative transverse momentum distributions (TMD), see e.g. [60] and references therein. TMDs contribute to the differential cross section predominantly at small transverse momenta of the DY pairs and for moderate masses of the pairs.

For large masses the theory works now very well providing a parameter free description of the Z -boson production at the LHC including the transverse momenta distribution.

Corresponding high precision data for fixed target energies are very limited especially for the antiproton projectiles. Fig. 5 shows the result of the model for $\bar{p}W$ collisions of the E537 collaboration at $s = 236\text{GeV}^2$ [61].

The data are compared with the model calculation [62] which includes pQCD parton evolution, and the TMD effects.

The model parameters have been fixed by using data on dimuon transverse-momentum spectra in pp collisions at $s = 1500\text{GeV}^2$ from the E866 collaboration in [64, 65]. This model describes the dimuon production data without any adjustment of model parameters quite well, in particular, the absolute cross section in pd collisions from the E772 collaboration [66], in pCu collisions from the E605 collaboration [67] at the same collision energy, as well as in pA collisions from the E288 collaboration [68] and in pW collisions from

the E439 collaboration [69] at $s = 750 \text{ GeV}^2$.

The presence of the abundant antiquarks and the forward kinematics experimental arm of PANDA at the HESR-C $\bar{p}p$ collider allows to determine the minimal M^2 for which the DY mechanism works. (Note that the charm contribution is strongly suppressed at $x_p \geq 0.4$ as a lepton in a charm decay carries, on average, only 1/3 of the D-meson momentum (and even less for charm baryons)).

The onset of factorization in the DY process with nuclei has still not been explored, but will be very interesting. Indeed, as mentioned already, the formation length in these processes is pretty small. Hence, one could think of the process in a semiclassical way, for a rather broad range of energies. In this picture, in the case of a nuclear target, the antiproton may experience one or more (in)elastic rescatterings on the target nucleons – before it annihilates with a proton into a dilepton pair. This effect can be taken into account within transport models, e.g. GiBUU [70] calculations, which are a good setup for the antiproton-nucleus dynamics. The antiproton stopping shall lead to a softening of the invariant-mass and transverse-momentum spectra of the dilepton pairs. It is also important to include these effects in future calculations, as it influences the conclusions on the in-medium modifications of the nucleon PDFs.

At high enough energies the formation time becomes large, but an antiquark which is involved in the DY process can experience energy losses growing quadratically with the path length [71]. Here one expects p_T broadening $\propto A^{1/3}$. These studies, if performed as a function of the atomic number and of the collision energy at fixed $x_{\bar{q}}$, may allow to explore these important effects in great detail.

6 Final remarks

The exciting science discussed here could be extended to much higher energies and heavier states if – in a later phase of FAIR – one can manage to reinject antiprotons from the HESR into one or two of the higher energy main FAIR synchrotrons, SIS 100 and SIS 300. Then $\bar{p}A$ collisions can be synchronized to run effectively and with high luminosity in a collider mode too. Also, crossing beams of SIS100 with SIS300, e.g. 45 AGeV heavy ions in the SIS 300 colliding with 30 GeV antiprotons (or protons), or with ions of 15 AGeV in the SIS100 can be envisioned. Also other asymmetric collisions maybe

feasible, e.g., 90 GeV antiprotons/protons (SIS300) colliding with 15 AGeV heavy ions (or with 30 GeV protons or antiprotons), in the SIS 100.

Acknowledgments

We thank M. Cacciari and R. Vogt for discussions on charm and beauty production in $\bar{p}p$ scattering. Research of L.F. and M.S. was supported by the US Department of Energy Office of Science, Office of Nuclear Physics under Award No. DE-FG02-93ER40771. A.L. acknowledges partial financial support by Helmholtz International Center (HIC) for FAIR. H.v.H. acknowledges the support from Frankfurt Institute for Advanced Studies (FIAS). H.St. acknowledges the support through the Judah M. Eisenberg Laureatus Chair by Goethe University and the Walter Greiner Gesellschaft, Frankfurt.

References

- [1] J. E. Augustin et al. (SLAC-SP-017 Collaboration), Discovery of a Narrow Resonance in e^+e^- Annihilation, *Phys. Rev. Lett.* **33**, 1406 (1974), <http://dx.doi.org/10.1103/PhysRevLett.33.1406>.
- [2] J. J. Aubert et al. (E598 Collaboration), Experimental Observation of a Heavy Particle J, *Phys. Rev. Lett.* **33**, 1404 (1974), <http://dx.doi.org/10.1103/PhysRevLett.33.1404>.
- [3] S. W. Herb et al., Observation of a Dimuon Resonance at 9.5 GeV in 400 GeV Proton-Nucleus Collisions, *Phys. Rev. Lett.* **39**, 252 (1977), <http://dx.doi.org/10.1103/PhysRevLett.39.252>.
- [4] H. Stöcker, T. Stöhlker, and C. Sturm, FAIR - Cosmic Matter in the Laboratory, *J. Phys. Conf. Ser.* **623**, 012026 (2015), <http://dx.doi.org/10.1088/1742-6596/623/1/012026>.
- [5] V. Barone et al. (PAX Collaboration), Antiproton-proton scattering experiments with polarization (2005), [arXiv:hep-ex/0505054](http://arxiv.org/hep-ex/0505054), <http://arxiv.org/hep-ex/0505054>.
- [6] PAX Collaboration, Technical Proposal for Antiproton-Proton Scattering Experiments with Polarization, Tech. rep.,

- Forschungszentrum Jülich (2006),
http://collaborations.fz-juelich.de/ikp/pax/public_files/proposals/techproposal20060125.pdf.
- [7] A. Lehrach, Accelerator Configuration for Polarized Proton-Antiproton Physics at FAIR, AIP Conference Proceedings **915**, 147 (2007).
- [8] I. N. Mishustin, L. M. Satarov, J. Schaffner, H. Stöcker, and W. Greiner, Baryon anti-baryon pair production in strong meson fields, J. Phys. G **19**, 1303 (1993),
<http://dx.doi.org/10.1088/0954-3899/19/9/009>.
- [9] A. B. Larionov, I. N. Mishustin, L. M. Satarov, and W. Greiner, Dynamical simulation of bound antiproton-nuclear systems and observable signals of cold nuclear compression, Phys. Rev. C **78**, 014604 (2008), <http://dx.doi.org/10.1103/PhysRevC.78.014604>.
- [10] F. Bradamante, I. Koop, A. Otboev, V. Parkhomchuk, V. Reva, P. Shatunov, and Y. Shatunov, Conceptual design for a polarized proton-antiproton collider facility at GSI (2005),
[arXiv:physics/0511252](http://arxiv.org/abs/physics/0511252), <http://arxiv.org/abs/physics/0511252>.
- [11] A. Lehrach, O. Boine-Frankenheim, F. Hinterberger, R. Maier, and D. Prasuhn, Beam performance and luminosity limitations in the high-energy storage ring (HESR), Nucl. Instrum. Meth. A **561**, 289 (2006), <http://dx.doi.org/10.1016/j.nima.2006.01.017>.
- [12] P. Beller, K. Beckert, C. Dimopoulou, A. Dolinsky, F. Nolden, M. Steck, and J. Yang, Layout of an accumulator and decelerator ring for FAIR, Conf. Proc. C **060626**, 199 (2006), <http://accelconf.web.cern.ch/AccelConf/e06/PAPERS/MOPCH074.PDF>.
- [13] V. V. Parkhomchuk, V. B. Reva, A. N. Skrinsky, V. A. Vostrikov, K. Beckert, P. Beller, A. Dolinskii, B. Franzke, F. Nolden, and M. Steck, An Electron Cooling System for the Proposed HESR Antiproton Storage Ring, in *9th European Particle Accelerator Conference (EPAC 2004) Lucerne, Switzerland, July 5-9, 2004* (2004),
<http://accelconf.web.cern.ch/AccelConf/e04/PAPERS/WEPLT056.PDF>.

- [14] D. Reistad et al., Status of the HESR electron cooler design work, Conf. Proc. C **060626**, 1648 (2006).
- [15] V. Kamerdzhiev et al., 2 MeV Electron Cooler for COSY and HESR – First Results, in *Proceedings, 5th International Particle Accelerator Conference (IPAC 2014): Dresden, Germany, June 15-20, 2014*, MOPRI070 (2014), <http://jacow.org/IPAC2014/papers/mopri070.pdf>.
- [16] M. Karliner, Heavy exotic quarkonia and doubly heavy baryons, EPJ Web Conf. **96**, 01019 (2015).
- [17] M. Cacciari, P. Nason, and C. Oleari, A Study of heavy flavored meson fragmentation functions in e^+e^- annihilation, JHEP **04**, 006 (2006), <http://dx.doi.org/10.1088/1126-6708/2006/04/006>.
- [18] M. Beneke, A. P. Chapovsky, M. Diehl, and T. Feldmann, Soft collinear effective theory and heavy to light currents beyond leading power, Nucl. Phys. B **643**, 431 (2002), [arXiv:hep-ph/0206152](https://arxiv.org/abs/hep-ph/0206152), [http://dx.doi.org/10.1016/S0550-3213\(02\)00687-9](http://dx.doi.org/10.1016/S0550-3213(02)00687-9).
- [19] M. Cacciari and R. Vogt, private communications.
- [20] M. Tanabashi et al. (Particle Data Group), The Review of Particle Physics (2018), Phys. Rev. D **98**, 030001 (2018), <http://pdg.lbl.gov/>.
- [21] G. D. Alkhazov, S. L. Belostotsky, and A. A. Vorobev, Scattering of 1-GeV Protons on Nuclei, Phys. Rept. **42**, 89 (1978), [http://dx.doi.org/10.1016/0370-1573\(78\)90083-2](http://dx.doi.org/10.1016/0370-1573(78)90083-2).
- [22] A. B. Larionov and H. Lenske, Elastic scattering, polarization and absorption of relativistic antiprotons on nuclei, Nucl. Phys. A **957**, 450 (2017), <http://dx.doi.org/10.1016/j.nuclphysa.2016.10.006>.
- [23] I. V. Moskalenko, A. W. Strong, J. F. Ormes, and M. S. Potgieter, Secondary anti-protons and propagation of cosmic rays in the galaxy and heliosphere, Astrophys. J. **565**, 280 (2002), <http://dx.doi.org/10.1086/324402>.

- [24] A. A. Tyapkin, A possible way of establishing the existence of charmed particles, *Sov. J. Nucl. Phys.* **22**, 89 (1976).
- [25] C. B. Dover and S. H. Kahana, Possibility of Charmed Hypernuclei, *Phys. Rev. Lett.* **39**, 1506 (1977),
<http://dx.doi.org/10.1103/PhysRevLett.39.1506>.
- [26] K. Tsushima and F. C. Khanna, Lambda(c)+ and Lambda(b) hypernuclei, *Phys. Rev. C* **67**, 015211 (2003),
<http://dx.doi.org/10.1103/PhysRevC.67.015211>.
- [27] A. B. Larionov and H. Lenske, Distillation of scalar exchange by coherent hypernucleus production in antiproton-nucleus collisions, *Phys. Lett. B* **773**, 470 (2017),
<http://dx.doi.org/10.1016/j.physletb.2017.09.007>.
- [28] R. Shyam and K. Tsushima, Production of Λ_c^+ hypernuclei in antiproton - nucleus collisions, *Phys. Lett. B* **770**, 236 (2017),
<http://dx.doi.org/10.1016/j.physletb.2017.04.057>.
- [29] L. Gerland, L. Frankfurt, M. Strikman, H. Stöcker, and W. Greiner, J/ψ production, χ polarization and color fluctuations, *Phys. Rev. Lett.* **81**, 762 (1998), [arXiv:nuc1-th/9803034](https://arxiv.org/abs/nuc1-th/9803034),
<http://dx.doi.org/10.1103/PhysRevLett.81.762>.
- [30] L. L. Frankfurt and M. I. Strikman, Point-like configurations in hadrons and nuclei and deep inelastic reactions with leptons: EMC and EMC-like effects, *Nucl. Phys. B* **250**, 143 (1985),
[http://dx.doi.org/10.1016/0550-3213\(85\)90477-8](http://dx.doi.org/10.1016/0550-3213(85)90477-8).
- [31] M. Alvioli, B. A. Cole, L. Frankfurt, D. V. Perepelitsa, and M. Strikman, Evidence for x -dependent proton color fluctuations in pA collisions at the CERN Large Hadron Collider, *Phys. Rev. C* **93**, 011902 (2016), <http://dx.doi.org/10.1103/PhysRevC.93.011902>.
- [32] M. Alvioli, L. Frankfurt, D. Perepelitsa, and M. Strikman, Global analysis of color fluctuation effects in proton- and deuteron-nucleus collisions at RHIC and the LHC (2017),
<http://arXiv.org/abs/1709.04993>.

- [33] L. Van Hove and S. Pokorski, High-Energy Hadron-Hadron Collisions and Internal Hadron Structure, Nucl. Phys. B **86**, 243 (1975), [http://dx.doi.org/10.1016/0550-3213\(75\)90443-5](http://dx.doi.org/10.1016/0550-3213(75)90443-5).
- [34] S. Raha, Dilepton, diphoton and photon production in preequilibrium, Phys. Scripta **T32**, 180 (1990), <http://dx.doi.org/10.1088/0031-8949/1990/T32/030>.
- [35] E. V. Shuryak, Two stage equilibration in high-energy heavy ion collisions, Phys. Rev. Lett. **68**, 3270 (1992), <http://dx.doi.org/10.1103/PhysRevLett.68.3270>.
- [36] J. Alam, B. Sinha, and S. Raha, Successive equilibration in quark - gluon plasma, Phys. Rev. Lett. **73**, 1895 (1994).
- [37] T. S. Biro, E. van Doorn, B. Muller, M. H. Thoma, and X. N. Wang, Parton equilibration in relativistic heavy ion collisions, Phys. Rev. C **48**, 1275 (1993), <http://dx.doi.org/10.1103/PhysRevC.48.1275>.
- [38] D. M. Elliott and D. H. Rischke, Chemical equilibration of quarks and gluons at RHIC and LHC energies, Nucl. Phys. A **671**, 583 (2000), [http://dx.doi.org/10.1016/S0375-9474\(99\)00840-4](http://dx.doi.org/10.1016/S0375-9474(99)00840-4).
- [39] Z. Xu and C. Greiner, Thermalization of gluons in ultrarelativistic heavy ion collisions by including three-body interactions in a parton cascade, Phys. Rev. C **71**, 064901 (2005), <http://dx.doi.org/10.1103/PhysRevC.71.064901>.
- [40] H. Stöcker et al., Glueballs amass at RHIC and LHC Colliders! - The early quarkless 1st order phase transition at $T = 270$ MeV - from pure Yang-Mills glue plasma to GlueBall-Hagedorn states, J. Phys. G **43**, 015105 (2016), <http://dx.doi.org/10.1088/0954-3899/43/1/015105>.
- [41] H. Stöcker et al., Undersaturation of quarks at early stages of relativistic nuclear collisions: The hot glue initial scenario and its observable signatures, Astron. Nachr. **336** (2015), <http://dx.doi.org/10.1002/asna.201512252>.
- [42] S. Borsanyi, G. Endrodi, Z. Fodor, S. D. Katz, and K. K. Szabo, Precision SU(3) lattice thermodynamics for a large temperature range,

- JHEP **07**, 056 (2012), 1204.6184,
[http://dx.doi.org/10.1007/JHEP07\(2012\)056](http://dx.doi.org/10.1007/JHEP07(2012)056).
- [43] M. Beitel, C. Greiner, and H. Stöcker, Fast dynamical evolution of a hadron resonance gas via Hagedorn states, Phys. Rev. C **94**, 021902 (2016), <http://dx.doi.org/10.1103/PhysRevC.94.021902>.
- [44] V. Vovchenko, M. I. Gorenstein, L. M. Satarov, I. N. Mishustin, L. P. Csernai, I. Kisel, and H. Stöcker, Entropy production in chemically nonequilibrium quark-gluon plasma created in central Pb+Pb collisions at energies available at the CERN Large Hadron Collider, Phys. Rev. C **93**, 014906 (2016), <http://dx.doi.org/10.1103/PhysRevC.93.014906>.
- [45] V. Vovchenko, I. A. Karpenko, M. I. Gorenstein, L. M. Satarov, I. N. Mishustin, B. Kämpfer, and H. Stöcker, Electromagnetic probes of a pure-gluon initial state in nucleus-nucleus collisions at energies available at the CERN Large Hadron Collider, Phys. Rev. C **94**, 024906 (2016), <http://dx.doi.org/10.1103/PhysRevC.94.024906>.
- [46] V. Vovchenko, L.-G. Pang, H. Niemi, I. A. Karpenko, M. I. Gorenstein, L. M. Satarov, I. N. Mishustin, B. Kämpfer, and H. Stöcker, Hydrodynamic modeling of a pure-gluon initial scenario in high-energy hadron and heavy-ion collisions, PoS **BORMIO2016**, 039 (2016).
- [47] I. Karpenko, P. Huovinen, and M. Bleicher, A 3+1 dimensional viscous hydrodynamic code for relativistic heavy ion collisions, Comput. Phys. Commun. **185**, 3016 (2014), <http://dx.doi.org/10.1016/j.cpc.2014.07.010>.
- [48] S. Borsanyi, Z. Fodor, C. Hoelbling, S. D. Katz, S. Krieg, and K. K. Szabo, Full result for the QCD equation of state with 2+1 flavors, Phys. Lett. B **730**, 99 (2014), <http://dx.doi.org/10.1016/j.physletb.2014.01.007>.
- [49] V. Vovchenko, *Quantum statistical van der Waals equation and its QCD applications*, Ph.D. thesis, Goethe University Frankfurt (2018).
- [50] R. Rapp and J. Wambach, Low mass dileptons at the CERN SPS: Evidence for chiral restoration?, Eur. Phys. J. A **6**, 415 (1999), <http://dx.doi.org/10.1007/s100500050364>.

- [51] R. Rapp, J. Wambach, and H. van Hees, The Chiral Restoration Transition of QCD and Low Mass Dileptons, *Landolt-Börnstein* **23**, 134 (2010), http://dx.doi.org/10.1007/978-3-642-01539-7_6.
- [52] S. Endres, H. van Hees, and M. Bleicher, Photon and dilepton production at the Facility for Proton and Anti-Proton Research and beam-energy scan at the Relativistic Heavy-Ion Collider using coarse-grained microscopic transport simulations, *Phys. Rev. C* **93**, 054901 (2016), <http://dx.doi.org/10.1103/PhysRevC.93.054901>.
- [53] T. Galatyuk, P. M. Hohler, R. Rapp, F. Seck, and J. Stroth, Thermal Dileptons from Coarse-Grained Transport as Fireball Probes at SIS Energies, *Eur. Phys. J. A* **52**, 131 (2016), <http://dx.doi.org/10.1140/epja/i2016-16131-1>.
- [54] J. Staudenmaier, J. Weil, V. Steinberg, S. Endres, and H. Petersen, Dilepton production and resonance properties within a new hadronic transport approach in the context of the GSI-HADES experimental data (2017), [arXiv:1711.10297\[nucl-th\]](https://arxiv.org/abs/1711.10297).
- [55] O. Linnyk, E. L. Bratkovskaya, and W. Cassing, Effective QCD and transport description of dilepton and photon production in heavy-ion collisions and elementary processes, *Prog. Part. Nucl. Phys.* **87**, 50 (2016), <http://dx.doi.org/10.1016/j.pnpnp.2015.12.003>.
- [56] M. Glück, E. Reya, and A. Vogt, Dynamical parton distributions of the proton and small x physics, *Z. Phys. C* **67**, 433 (1995), <http://dx.doi.org/10.1007/BF01624586>.
- [57] M. Gluck, E. Reya, and A. Vogt, Pionic parton distributions, *Z. Phys. C* **53**, 651 (1992), <http://dx.doi.org/10.1007/BF01559743>.
- [58] C. Spieles, L. Gerland, N. Hammon, M. Bleicher, S. A. Bass, H. Stöcker, W. Greiner, C. Lourenco, and R. Vogt, A Microscopic calculation of secondary Drell-Yan production in heavy ion collisions, *Eur. Phys. J. C* **5**, 349 (1998), <http://dx.doi.org/10.1007/s100520050279>.
- [59] C. Spieles, L. Gerland, N. Hammon, M. Bleicher, S. A. Bass, H. Stöcker, W. Greiner, C. Lourenco, and R. Vogt, Intermediate mass

- dileptons from secondary Drell-Yan processes, Nucl. Phys. A **638**, 507 (1998), [http://dx.doi.org/10.1016/S0375-9474\(98\)00345-5](http://dx.doi.org/10.1016/S0375-9474(98)00345-5).
- [60] R. Angeles-Martinez et al., Transverse Momentum Dependent (TMD) parton distribution functions: status and prospects, Acta Phys. Polon. B **46**, 2501 (2015), <http://dx.doi.org/10.5506/APhysPolB.46.2501>.
- [61] E. Anassontzis et al., High mass dimuon production in $\bar{p}n$ and π^-n interactions at 125-GeV/c, Phys. Rev. D **38**, 1377 (1988), <http://dx.doi.org/10.1103/PhysRevD.38.1377>.
- [62] F. Eichstaedt, S. Leupold, K. Gallmeister, H. van Hees, and U. Mosel, Description of Fully Differential Drell-Yan Pair Production, PoS **BORMIO2011**, 042 (2011), [arXiv:1108.5287](https://arxiv.org/abs/1108.5287) [hep-ph].
- [63] A. D. Martin, W. J. Stirling, R. S. Thorne, and G. Watt, Parton distributions for the LHC, Eur. Phys. J. C **63**, 189 (2009), <http://dx.doi.org/10.1140/epjc/s10052-009-1072-5>.
- [64] J. C. Webb et al. (NuSea Collaboration), Absolute Drell-Yan dimuon cross-sections in 800 GeV/c pp and pd collisions (2003), [arXiv:hep-ex/0302019](https://arxiv.org/abs/hep-ex/0302019).
- [65] J. C. Webb, *Measurement of continuum dimuon production in 800 GeV/c proton nucleon collisions*, Ph.D. thesis, New Mexico State U. (2003), [arXiv:hep-ex/0301031](https://arxiv.org/abs/hep-ex/0301031), <http://dx.doi.org/10.2172/1155678>.
- [66] P. L. McGaughey et al. (E772 Collaboration), Cross-sections for the production of high mass muon pairs from 800-GeV proton bombardment of H-2, Phys. Rev. D **50**, 3038 (1994), [Erratum: Phys. Rev.D60,119903(1999)], <http://dx.doi.org/10.1103/PhysRevD.50.3038>, [10.1103/PhysRevD.60.119903](https://arxiv.org/abs/10.1103/PhysRevD.60.119903).
- [67] G. Moreno et al., Dimuon production in proton - copper collisions at $\sqrt{s} = 38.8$ GeV, Phys. Rev. D **43**, 2815 (1991), <http://dx.doi.org/10.1103/PhysRevD.43.2815>.

- [68] A. S. Ito et al., Measurement of the Continuum of Dimuons Produced in High-Energy Proton - Nucleus Collisions, Phys. Rev. D **23**, 604 (1981), <http://dx.doi.org/10.1103/PhysRevD.23.604>.
- [69] S. R. Smith et al., Experimental Test of the Drell-Yan Model in $pW \rightarrow \mu^+\mu^-X$, Phys. Rev. Lett. **46**, 1607 (1981), <http://dx.doi.org/10.1103/PhysRevLett.46.1607>.
- [70] O. Buss, T. Gaitanos, K. Gallmeister, H. van Hees, M. Kaskulov, et al., Transport-theoretical Description of Nuclear Reactions, Phys. Rept. **512**, 1 (2012), <http://dx.doi.org/10.1016/j.physrep.2011.12.001>.
- [71] R. Baier, Y. L. Dokshitzer, A. H. Mueller, S. Peigne, and D. Schiff, Radiative energy loss and $p(T)$ broadening of high-energy partons in nuclei, Nucl. Phys. B **484**, 265 (1997), [http://dx.doi.org/10.1016/S0550-3213\(96\)00581-0](http://dx.doi.org/10.1016/S0550-3213(96)00581-0).